Clays and Clay Minerals, Vol. 36, No. 2, 102–110, 1988.

FERRIAN SAPONITE IN A GABBRO SAPROLITE AT MONT MÉGANTIC, QUEBEC

H. KODAMA,[1] C. R. DE KIMPE,[1] AND J. DEJOU[2]

[1] Land Resource Research Centre, Agriculture Canada
Ottawa, Ontario K1A 0C6, Canada

[2] INRA, Station d'Agronomie, 12 Avenue de l'Agriculture
63039 Clermont Ferrand Cedex, France

Abstract—Gabbroic saprolite at Mont Mégantic, Quebec, was studied in detail mineralogically to gain a better understanding of the origin of ferruginous smectite reported previously from these rocks. The parent rock is a ferrogabbro composed of plagioclase, augite, calc-alkalic amphiboles, biotite, olivine, magnetite, ilmenite, and apatite. Extensive weathering has decomposed most of the mafic minerals and magnetite to goethite, lepidocrocite, and iron-rich clay minerals, which occur in numerous microcracks distributed irregularly in the outer shells of boulders and in cracks and fissures in the bedrock. Some of the felsic minerals have altered to kaolinite. The secondary minerals and the more resistant primary minerals, such as plagioclase, ilmenite, and apatite, have subsequently moved to the lower part of the saprolite. The major ferruginous clay minerals present are smectite and vermiculite, which are compositionally similar, except that the smectite is slightly richer in SiO_2 and MgO and poorer in Fe_2O_3 than the vermiculite.

To establish a structural formula for the ferruginous smectite, the oxidation state of Fe in a sample treated with dithionite-citrate-bicarbonate was examined by Mössbauer spectroscopy. All structural iron was found to be ferric. The calculated structural formula of a Na-saturated sample is:

$$Na_{0.61}(Mg_{1.39}Fe^{3+}_{0.85}Al_{0.17}Mn_{0.03})(Si_{3.49}Al_{0.51})O_{10}(OH)_2,$$

which has a total octahedral population of 2.44. Octahedral (Mg + Mn) exceeds octahedral (Fe^{3+} + Al). The 060 reflection at 1.527 Å is closer to the 1.530-Å value typical of saponite than to the 1.518-Å value typical of nontronite. The infrared spectra of the ferruginous smectite is also similar to that of saponite. Thus, the mineral is best described as a ferrian saponite. Ferroan saponite originally formed, and due to subsequent oxidation, some Fe^{3+} was expelled from the octahedral sheets, giving rise to a ferrian saponite containing octahedral vacancies. The expelled iron presumably formed the iron oxyhydroxides that coexist with the saponite.

Key Words—Ferric iron, Genesis, Oxidation, Saponite, Saprolite, Weathering.

INTRODUCTION

Reid (1976) studied the geology of Mont Mégantic in the Appalachian Highlands, Quebec, and reported gabbroic intrusions between the outer syenite rim and the inner granitic core of the mountain. The gabbros are lower Cretaceous in age on the basis of fission track dating and Rb/Sr data from apatites, which indicate 134 and 133 m.y., respectively (Eby, 1984). Clément and De Kimpe (1977) reported a nontronitic smectite as the major secondary mineral in the clay-size fraction of a saprolite developed on the gabbro. Kodama and De Kimpe (1983) found that this particular smectite was both ferruginous and magnesian, and that it contained significant Al substituting for Si. At that stage of research, they were unable to classify the mineral as either a nontronite or saponite.

The occurrence of ferruginous smectite minerals as alteration products of basic igneous rocks has been reported several times (e.g., Sudo, 1954; Miyamoto, 1957; Sherman *et al.*, 1962; Delvigne *et al.*, 1979). The specific information concerning these clay minerals, however, has often been inconclusive because of the difficulty in interpreting correctly the chemical data or possibly because of the presence of impurities or the rapid oxidation of Fe^{2+} in the structure. Kohyama *et al.* (1973) studied in detail iron-rich saponite derived from rhyolitic glassy tuffs and explained the existence of saponites rich in ferrous and ferric iron by assuming a ferrous analogue of saponite as an end-member.

This hypothesis appears to be particularly applicable to smectites rich in Mg and Fe, such as the ferruginous smectite found in the Mont Mégantic gabbroic saprolite. Therefore, a closer examination of the alteration of the saprolite with respect to the the formation of the ferruginous smectite appeared to be warranted. The results of this examination are presented in this report.

MATERIALS AND METHODS

The site is on the north side of Mont Mégantic, at 45°28′00″N and 71°8′30″W, as described previously by Clément and De Kimpe (1977). In 1982, a new cut, about 5 m wide and 4 m high, was examined. Twenty-two samples were collected from cracks and fissures (Figure 1) and kept moist in plastic bags to reduce Fe^{2+} oxidation as much as possible. Depending on the nature of the sample, fractionation procedures included grinding, sonification, and sedimentation. The clay-

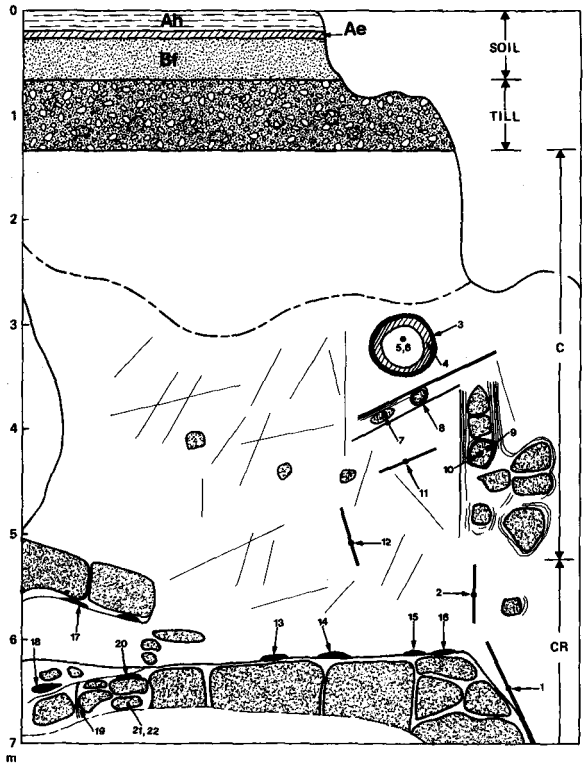

Figure 1. Schematic representation of alteration profile showing sample locations. Numbers for sample locations correspond to last one or two digits of sample numbers given in Table 1.

size samples (<2 μm) were saturated with Mg and freeze-dried. Iron oxides were removed from the clay fraction by the dithionite-citrate-bicarbonate (DCB) method (Mehra and Jackson, 1960) and determined by atomic absorption spectroscopy (AA). Coarse samples (<45 μm) were prepared by grinding.

For total chemical analysis, samples were dried overnight at 110°C. Silica was determined gravimetrically following decomposition by the Na_2CO_3 fusion method. Other elements were determined by AA after dissolution of subsamples by an HF-$HClO_4$ digestion method. Ferrous iron was determined by a back titration method (Reichen and Fahey, 1962). Loss on ignition was expressed by weight loss between 110° and 1000°. Total cation-exchange capacity was assessed from the amount of Mg cations displaced by Ca cations when the Mg-saturated samples were treated with 1 N $CaCl_2$.

Four techniques were used for X-ray powder diffraction (XRD) analysis. Using CoKα radiation, XRD patterns of non-oriented whole rock samples and of oriented and non-oriented clay-size samples were recorded using a Scintag PAD V automated powder diffractometer equipped with a graphite monochromator. The oriented samples were prepared by drying 30 mg of each sample suspended in 1 ml of H_2O on a 25 mm × 30 mm glass slide. Glycerolation was achieved by using 1 ml of 2% glycerol-water solution instead of H_2O in the procedure mentioned above. Small-size samples separated by a heavy liquid method according to specific gravity were analyzed with a Debye-Scherrer camera. Small mineral grains, removed with a needle and tweezers from rock thin sections after polarized-light microscopic observations, were analyzed using a Gandolfi camera. For the measurement of d(060), a Guinier-de Wolff camera was used. For all camera analyses except that using a Guinier-de Wolff camera, an Fe filter was used to monochromatize the primary X-rays.

Thin sections of rock samples, except for the relatively fresh gabbro (sample 82110), were prepared by embedding undisturbed samples in epoxy resin (Araldite). Small portions of these thin sections and aggregates of small mineral grain were examined by scanning electron microscopy using a Cambridge S4 stereoscan electron microscope (SEM). SEM examination was accompanied by elemental analysis by means of a Kevex energy-dispersive X-ray analyzer (EDX) that permitted spectrochemical analyses to supplement chemical and mineralogical data. Samples were also examined by transmission electron microscopy (TEM) using a Philips EM300 apparatus operated at 80 kV.

RESULTS AND DISCUSSION

Parent material

Table 1 briefly describes and lists the mineral assemblage of all samples examined. Based on its megascopic appearance, XRD data, and light-microscope observations, sample 82110 appears to be the least altered and perhaps the most representative parent rock material. The primary rock-forming minerals detected in this sample by XRD are plagioclase, clinopyroxene, calc-alkali amphiboles, biotite, olivine, magnetite, and ilmenite. Ilmenite was identified only in the magnetic fraction having a specific gravity >3.33. The 130 reflection of a small olivine crystal taken from a thin section was recorded at 2.800 Å. Using the equation established by Schwab and Küstner (1977), $X_{Fa} = 7.522 - 14.9071[3.0199 - d(130)]^{0.5}$, the composition of olivine in the gabbro was calculated to be about Fo_{47}. The composition of plagioclase was determined from the equation, $\beta = 2\theta(1\bar{1}1) - 2\theta(20\bar{1})$ for CuKα radiation (Smith and Gay, 1958) after converting the recorded 2θ (CoKα) values into their CuKα equivalents. The beta values for several plagioclase crystals gave an average composition of Ab_{60}.

Chemical compositions of a clinopyroxene and of a calcic amphibole were determined by EDX on a single grain of each mineral isolated from thin sections. The clinopyroxene composition, $(Ca_{0.42}Mg_{0.34}Fe_{0.21})SiO_3$, falls within the augite group, although it is near the

https://doi.org/10.1346/CCMN.1988.0360202 Published online by Cambridge University Press

Table 1. Physical description and mineral composition of 22 samples collected from Mont Mégantic, Quebec.

Sample	Description	Mineral composition of whole rock and/or clay[1]	Sample	Description	Mineral composition of whole rock and/or clay[1]
82101	Brown, soft fragments forming thin vein along fissure.	{sm + vm + lc + gt + v/m + (tc)}	82112	Similar to sample 82107, softer sample dark brown.	{vm + lc + ka + gt + (am)}
82102	Similar to sample 82101, but in dark gray color.	{sm + vm + v/m}	82113	Red-brown clayey sample.	{vm + lc + gt}
82103	Dark-brown rock fragments consisting of the outer shell of boulder.	{vm + sm + ka + tc + lc}	82114	Dark red-brown clayey sample.	{sm + lc}
82104	Dark-brown rock fragments consisting of the inner shell of boulder.	fs + am + vm {vm + sm + ka + lc}	82115	Red-brown clayey sample.	{sm + lc + gt + am}
82105	Blackish brown sample from the core of boulder (softer).	fs + vm + mi + am + vm + (sm)	82116	Red-brown clayey sample.	{vm + sm + lc + gt + (tc)}
82106	Blackish brown sample from the core of boulder (harder).	fs + am + mi + vm + (sm)	82117	Dark red-brown clayey sample.	{sm + vm + lc + gt}
82107	Ochre, small grain fragments forming thin vein along fissures.	fs + am + vm + (sm)	82118	Red-brown clayey sample.	{sm + vm + lc + gt}
82108	Dark-brown sample of the crust of a small gravel.	fs + vm + (sm)	82119	Dark-brown small rock fragments from thin vein along fissure.	am + fs + vm + (mi) {vm + sm + (mi)}
82109	Dark-brown, partially altered portion on the outer shell of a boulder.	fs + am + mi + (vm) + (sm) {sm + vm + ka + lc}	82120	Gray-brown softer sample near boulder.	sm + vm + ka + lc + (tc)
82110	Sample from a relatively fresh fracture of the boulder in saprolite.	fs + bt + am + px + ol + mt	82121	Dark red-brown rock fragments consisting of the outer shell of boulder.	fs + sm + (am) + (vm) {sm + (vm) + (tc)}
82111	Similar to sample 82107, harder sample, dark brown.	fs + am + (vm)	82122	Dark-gray rock, a relatively fresh portion of a saprolite boulder.	fs + am + mi

[1] { } denotes mineral composition of clay-size fraction. ( ) denotes that the quantity is very minor or trace. am = amphibole; bt = biotite; fs = feldspar; gt = goethite; il = ilmenite; ka = kaolinite; lc = lepidocrocite; mi = micas; mt = magnetite; ol = olivine; px = pyroxene; sm = smectite; tc = talc?, 9.3–9.4-Å phase; vm = vermiculite; v/m = vermiculite/mica interstratification.

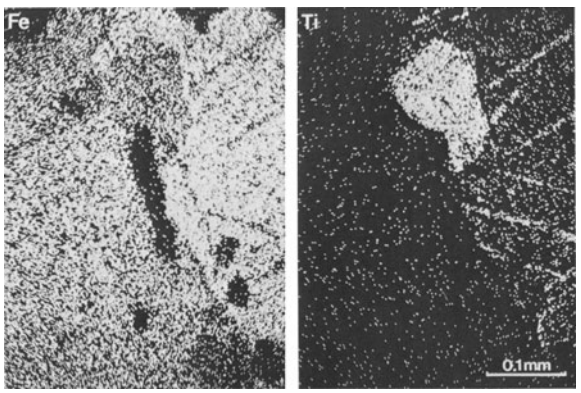

Figure 2. Energy-dispersive X-ray analysis of a thin section (sample 82105) showing isolated magnetite and ilmenite crystals and exsolution lamellae of ilmenite in magnetite matrix.

Table 2. Chemical composition (wt. %) of the relatively fresh parent gabbro, compared with an average composition of 41 gabbroic rocks.

	Mont Mégantic gabbro	Average[1]
SiO_2	46.20	48.24
TiO_2	2.61	0.97
Al_2O_3	15.69	17.88
Fe_2O_3	6.43	3.16
FeO	10.76	5.95
MnO	0.40	0.13
MgO	4.55	7.51
CaO	7.98	10.99
K_2O	0.37	0.89
Na_2O	4.23	2.55
L.O.I.	1.09	
Total	100.31	

[1] From *Handbook of Physical Constants* (Clark, 1966).

diopside-hedenbergite field. The calcic amphibole structural formula, $Ca_{1.9}(Fe_{3.4}Mg_{3.2})(Si_{7.0}Al_{1.0})O_{22}(OH)_2$, corresponds to a ferruginous tschermakite. Substantial amounts of magnetite and ilmenite in addition to the iron-rich mafic minerals described above suggest that the parent rock was a ferrogabbro. This identification is supported by the chemical analysis of the whole rock as compared with the average composition of 41 representative gabbros (Table 2). The Mont Mégantic sample contains nearly twice as much total iron as does this average. The ferrogabbro also contains a substantial amount of Ti. If all the TiO_2 is allocated to ilmenite, the ilmenite content would be 4.95%; however, ilmenite was not clearly identified by light microscopy, and it is therefore assumed to be intimately intermixed with magnetite. The EDX data appear to be more useful in detecting ilmenite, as exemplified in Figure 2, which shows isolated ilmenite crystals and exsolution lamellae of ilmenite in the magnetite matrix.

Saprolite

Highly altered rocks were collected from the outer shells of boulders and from veins and fissures (e.g., samples 82107, 82108, and 82111, Figure 1). Most of the mafic minerals present in the fresh rock were absent in the altered rocks, and feldspars were dominant components, along with various amounts of vermiculite and smectite. Minor amphibole was identified by XRD, whereas traces of olivine and pyroxene were only detected in some thin sections by optical microscopy. Goethite and lepidocrocite were found in the clay-size fractions of samples 82101 and 82112. Sample 82107, which appears to represent a relatively early stage of mineral weathering, was studied in more detail. Optical microscopic examination of the thin sections showed dark-red stains of microcrystalline material along cracks, fissures, and cleavages of residual minerals (see dark parts in sketch at top left of Figure 3). EDX analysis (Figure 3) indicates that the stains are almost exclusively iron (i.e., iron oxide or iron oxyhydroxide). These iron oxide or oxyhydroxide stains apparently resulted from the alteration of the mafic minerals and magnetite.

The EDX data from the same thin section (Figure 3) clearly indicated the presence of ilmenite and apatite. These minerals were also noted as isolated crystals coexisting with clay material in the lower part of the saprolite body (cf. Figure 5). Modes of occurrence of aggregates of secondary iron oxide or oxyhydroxide minerals were obtained by SEM and EDX analyses from the same sample (82107). At least two modes of occurrence were recognized: (1) on feldspar crystal surfaces (Figure 4a); and (2) as fillings in microcracks of feldspar crystals (Figure 4b).

Clay-size material

Clay-rich material (e.g., samples 82101, 82102, 82113–82118) is common at the bottom of the outcrop and in veins and cracks between resistant blocks of rock (Figure 1). Clay concentrations were collected from small pockets and depressions on the surface of relatively hard rocks. The clay material is brighter and redder than the other parts of the saprolite. SEM-EDX examination of unfractionated samples showed that clay-iron oxide mixtures locally contain residual minerals, such as feldspars, ilmenite, and apatite (Figure 5). This assemblage suggests that the resistant minerals, the clay material, and the iron oxides that formed in the upper part of the saprolite have moved to the lower part of the body. Typically, the clay-size fractions consist of smectite, vermiculite, lepidocrocite, and goethite, as identified by XRD. The glycerolated, Mg-saturated samples gave 18- and 14.4-Å XRD peaks, both of which shifted to 10 Å when the samples were heated at 550°C. The major XRD peaks of lepidocrocite and goethite at 6.25 and 4.18 Å, respectively, disappeared or were drastically reduced after the DCB treatment to remove iron oxide materials.

https://doi.org/10.1346/CCMN.1988.0360202 Published online by Cambridge University Press

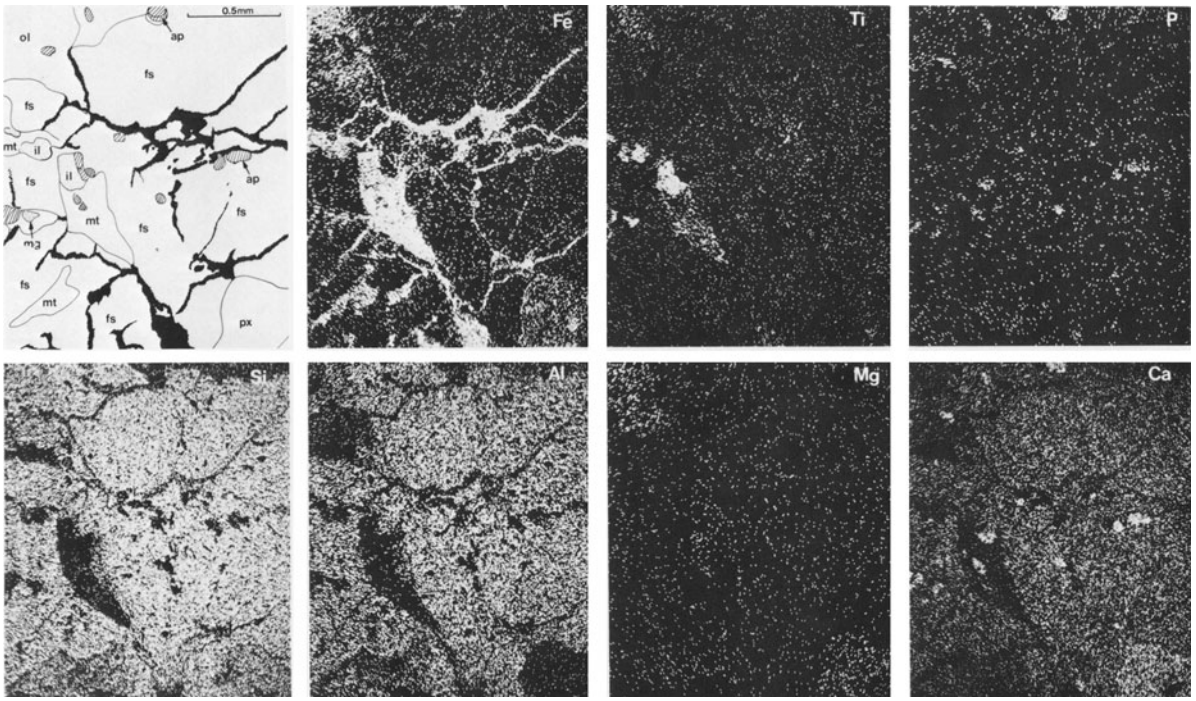

Figure 3. Energy-dispersive X-ray analysis of a thin section (sample 82107). In sketch at top left, black portions represent areas stained with dark red secondary iron oxide and dotted and shaded areas indicate those occupied by ilmenite and apatite, respectively. Abbreviations used in the sketch are the same as those used in Table 1.

In a few samples, trace to minor amounts of amphiboles, talc (or a talc-like mineral), kaolinite, and interstratified vermiculite/mica were detected. Kaolinite, in particular, was identified in the outer shells of boulders (samples 82103, 82104, and 82109) and in cracks (samples 82102 and 82112) in boulders that displayed good internal drainage, which allowed alkalis and silica to be leached. The presence and absence of kaolinite in a relatively small area may be related to environmental differences within that area, such as those described by Dejou *et al.* (1982) as microenvironmental effects. One of the goethite-bearing samples contained Al-free goethite, but the rest yielded 111 XRD reflections at 2.443–2.448 Å, indicative of Al substitution. Based on Norrish and Taylor's (1961) curve, these spacings correspond to 2–6 mole % Al substitution for Fe in the FeOOH structure. The significance of the Al substitution in the goethite is discussed below. In contrast, the (051, 200) XRD reflection of lepidocrocite was invariably at 1.941 Å, indicative of no Al substitution. Al substitution has not been reported for any natural lepidocrocites to date.

Expanding clay minerals

After treatment with DCB, samples 82114, 82117, and 82118 consisted almost entirely of expanding clay minerals. Sample 82114 contains chiefly smectite, sample 82117 consists chiefly of smectite with a minor amount of vermiculite, and sample 82118 consists chiefly of smectite plus more vermiculite than sample 82117. The expanding clay minerals occur as relatively well defined, thin, platy particles (Figure 6). These particles appear to be relatively free of crystal distortion, as indicated by the presence of only rare and weak diffuse streaks in micro-diffraction patterns. A relatively high thermal resistivity of the crystals was also indicated by the fact that the micro-diffraction spots,

Table 3. Chemical data[1] (wt. %) of dithionite-citrate-bicarbonate treated ferrian saponite (sample 82114)[2] and related samples.

Sample	82114	82117	82118
SiO_2	53.81	51.92	51.27
TiO_2	tr	tr	tr
Al_2O_3	8.89	9.07	9.43
Fe_2O_3[3]	17.54	22.23	23.50
MnO	0.46	0.34	0.35
MgO	14.39	11.17	9.52
CaO	0.02	0.07	0.14
Na_2O	4.88	5.18	5.77
K_2O	tr	0.01	0.02
CEC (meq/100 g)	96	97	—

[1] Based on ignited Na-saturated sample.
[2] Sample 82114 is the purest ferrian saponite among the three samples.
[3] Total iron.

https://doi.org/10.1346/CCMN.1988.0360202 Published online by Cambridge University Press

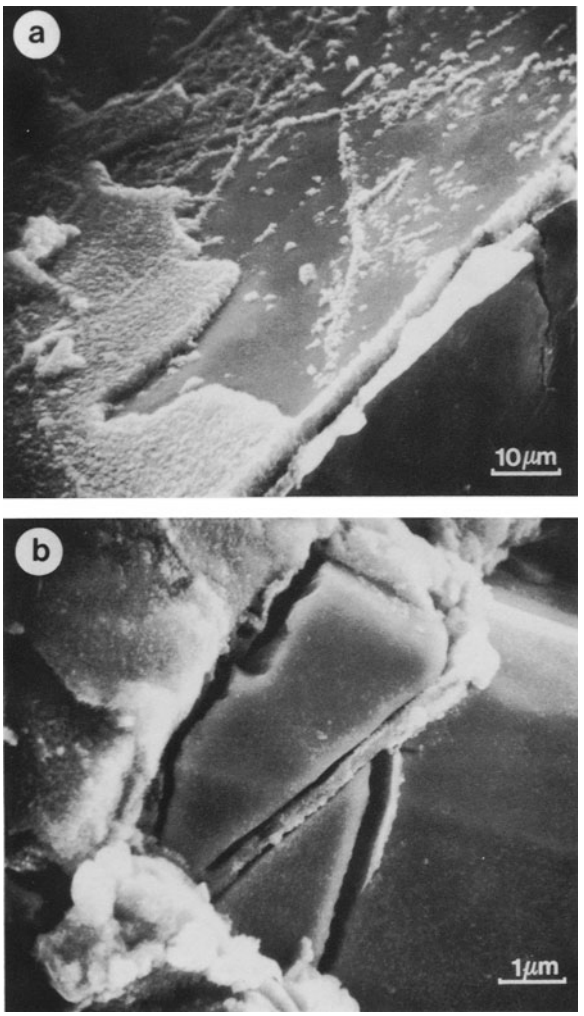

Figure 4. Scanning electron micrographs (sample 82107) showing secondary iron oxides (a) on a crystal surface of feldspar and (b) along cracks in a feldspar crystal.

like those inset in Figure 6, were noted even after continuous bombardment by the electron beam for at least 30 s. These features suggest that the expanding clay minerals are highly crystalline.

Chemical analyses of these three samples (Table 3) reflect the variations in mineralogical composition. The SiO_2 and MgO contents increase and the Fe_2O_3 content decreases with an increase in smectite, suggesting that the saponitic smectite is richer in SiO_2 and MgO and poorer in Fe_2O_3 than the vermiculite. These data are in good agreement with Weaver and Pollard's (1973) general ideas about the chemical composition of these two minerals.

Further characterization was required to account for the high Fe_2O_3 and MgO contents of the smectite. Due to large amounts of iron oxyhydroxide material (12–30% Fe) in the undeferrated samples, DCB-treated samples were used to assess chemical formulae. Because the residual reagent used in the DCB treatment caused erroneous reponse in the determination of Fe^{2+} by a back-titration method, the evaluation of Fe^{2+}/Fe^{3+} relied on Mössbauer spectra (not reported here) of the DCB-treated samples which showed a broad doublet having a narrow quadrupole splitting, indicating the absence of Fe^{2+}. Computations based on one paramagnetic component gave the following parameters: isomer shift = 0.32 mm/s (with respect to that of ^{57}Fe in iron foil); quadrupole splitting = 0.72 mm/s. These data are similar to the values of 0.38 mm/s and 0.6 mm/s, respectively, reported by Cardile and Johnston (1985) for an outer doublet, which corresponds to one of two doublets for cis-$FeO_4(OH)_2$ octahedral sites in nontronite.

Because complete solid solution has not been reported between nontronite and saponite, both minerals might be present in the above samples. Using a Guinier-de Wolff camera, the 060 reflection of nontronite at 1.518 Å clearly distinguishes it from saponite (d(060) = 1.530 Å), with a precision of 0.002 Å (see Figure 7). Applying this technique to DCB-treated samples 82114 and 82117 yielded a single reflection at 1.527 Å, close to the value for saponite, thereby ruling out the possibility of a mixture of the two minerals.

The similarity of these samples to saponite is further indicated by their infrared spectra (Kodama and De Kimpe, 1983; present study) which show no distinct absorption band near the characteristic nontronite band at 810–825 cm^{-1} (Moenke, 1966; Oinuma and Hayashi, 1968; Kodama, 1985). In saponite, a very small absorption band may exist in that region if the spectra are recorded on randomly oriented samples (Farmer, 1974). Thus, despite its high Fe_2O_3 content, the smectite gave an IR spectrum more closely resembling that of saponite than that of nontronite.

The following structural formula of the smectite was calculated on the basis of 22 negative charges from the chemical analysis of sample 82114 (Table 3):

Interlayer charge	octahedral charge	Deficiency in tetrahedral charge
+0.61	−0.10	−0.51
$Na_{0.61}$	$(Mg_{1.39}Fe^{3+}_{0.85}\cdot Al_{0.17}Mn_{0.03})$	$(Si_{3.49}\cdot Al_{0.51})O_{10}(OH)_2$

The total population of octahedral cations is 2.44, which at face value suggests an intermediate occupancy between dioctahedral and trioctahedral. Inasmuch as the sum of R^{2+} cations in octahedral sites is 1.42, which is less than 85% occupancy, and the sum of R^{3+} cations in the same sites is 1.02, which is greater than 0.5, the mineral cannot be classified as a typical trioctahedral smetite (Weaver and Pollard, 1973). On the other hand, although the mineral is iron-rich, the (Mg + Mn) content exceeds the (Fe^{3+} + Al) content in octahedral sites.

https://doi.org/10.1346/CCMN.1988.0360202 Published online by Cambridge University Press

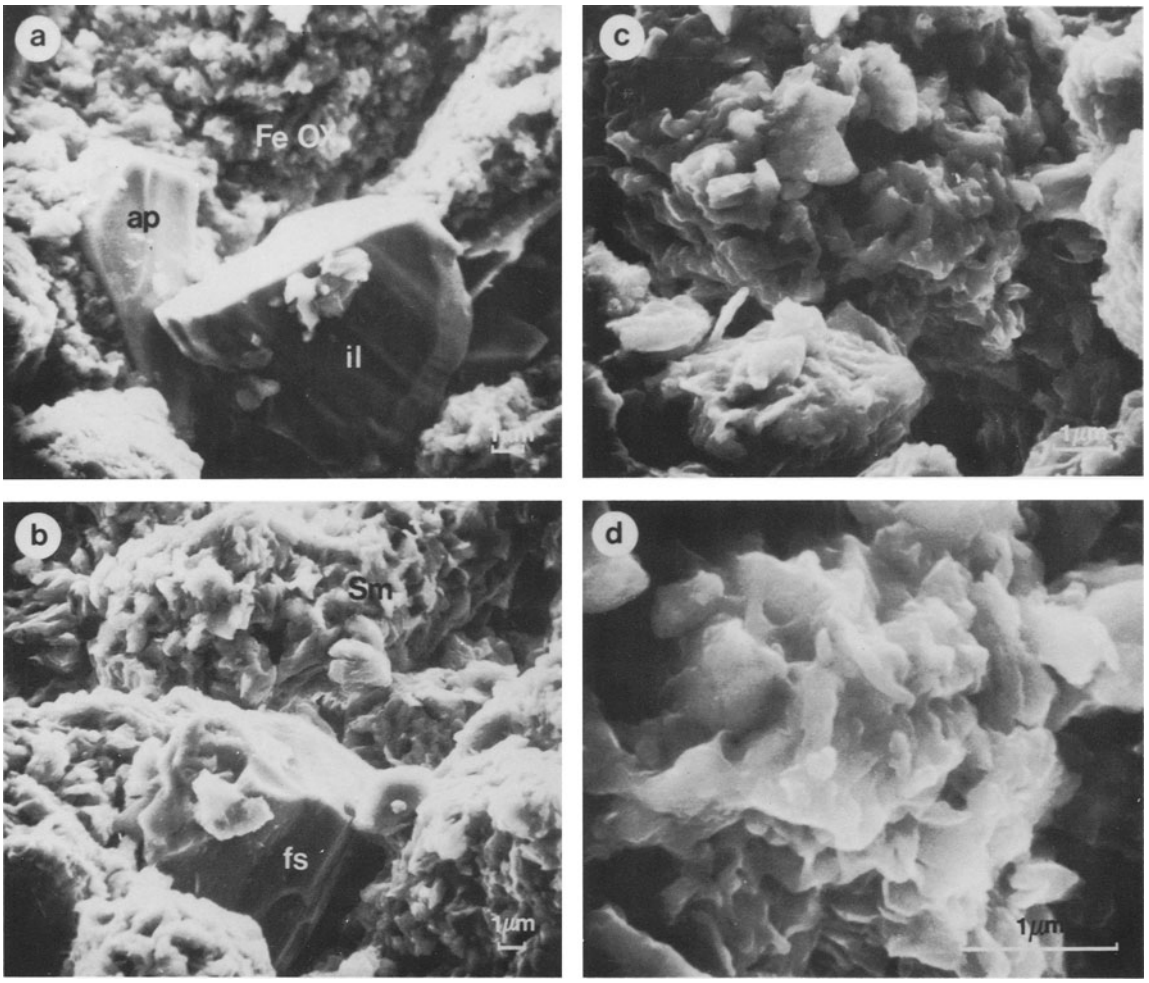

Figure 5. Scanning electron micrographs of clay-rich samples. (a) Secondary iron oxide minerals with ilmenite and apatite crystals, (b) ferruginous smectite with feldspar crystals, (c) ferruginous smectite, and (d) ferruginous smectite; enlargement of (c).

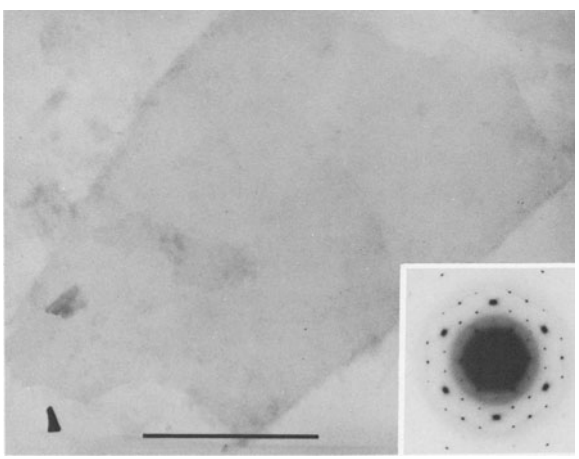

Figure 6. Transmission electron micrograph of the ferruginous smectite and corresponding electron diffraction pattern. Bar indicates 1 μm.

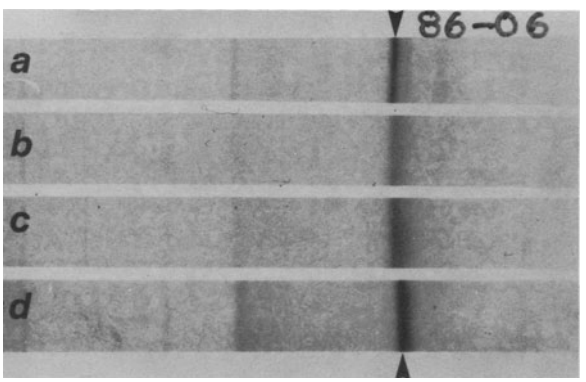

Figure 7. Portion of Guinier-de Wolff diffraction film showing 060 reflections of (b) sample 82114 and (c) sample 82117 compared with those of (a) saponite from Germany and (d) nontronite from State of Washington.

https://doi.org/10.1346/CCMN.1988.0360202 Published online by Cambridge University Press

On this basis, and on the basis of the 060 spacing (*vide supra*), the mineral is a magnesian smectite, closer to saponite than to nontronite. Iron-rich saponites have been reported by several investigators (e.g., Sudo and Ota, 1952; Sudo, 1954; Kohyama *et al.*, 1973). Kohyama *et al.* (1973) predicted the existence of the iron-analogue of saponite with the following ideal structural formula:

$$M^{+}_{0.33}(Fe^{2+}_{3})(Si_{3.67}Al_{0.33})O_{10}(OH)_2.$$

The genesis of the Mont Mégantic smectite mineral may be explained using the concept of a precursor ferroan saponite on the basis of the following steps:

1. The initial formation of a ferrous, iron-rich saponite.
2. The oxidation of Fe^{2+} ions by deprotonation of structural hydroxyls.
3. The restoration of hydroxyls by the reversible protonation of O^{2-}, derived from the previous deprotonation of OH ions.
4. The expulsion of Fe^{3+} ions from octahedral sites as a consequence of this OH restoration, thereby causing vacancies in the octahedral sheets.
5. The precipitation of ferric oxyhydroxides.

No cationic changes, except for iron, took place in the octahedral or tetrahedral sheets throughout the process. The Fe^{2+} content of the initial iron-rich saponite was determined by the total layer-charge balance after the interlayer charge of the iron-rich saponite was fixed at 0.34. According to this model, the process for the formation of Mont Mégantic ferric iron-rich saponite may be expressed by the following equation:

$$M^{+}_{0.34}(Mg_{1.39}Fe^{2+}_{1.41}Al_{0.17}Mn_{0.03})(Si_{3.49}Al_{0.51})O_{10}(OH)_2 \rightarrow M^{+}_{0.34}(Mg_{1.39}Fe^{3+}_{1.41}Al_{0.17}Mn_{0.03})(Si_{3.49}Al_{0.51})O_{11.41}(OH)_{0.59} + 1.41\ H^{+} \rightarrow M^{+}_{0.61}(Mg_{1.39}Fe^{3+}_{0.85}Al_{0.17}Mn_{0.03}\square_{0.56})(Si_{3.49}Al_{0.51})O_{10}(OH)_2 + 0.56\ FeO(OH),$$

where □ indicates vacancies.

Deprotonation of structural hydroxyls was demonstrated by Farmer *et al.* (1971) in a study of the experimental oxidation of biotites and vermiculites. Release of Fe^{3+} ions from the octahedral sheets of smectite in conjunction with a possibly Al-rich environment due to the alteration of primary minerals may have been responsible for the crystallization of the Al-substituted goethite at Mont Mégantic, as reported above. The absence of Al in the lepidocrocite, on the other hand, may be explained in terms of the rate of hydrolysis of Fe^{3+} ions. According to Schwertmann and Taylor (1977), goethite is produced by the slow hydrolysis of Fe^{3+} ions, whereas lepidocrocite is a product of fast hydrolysis under hydromorphic and partly reducing conditions. Therefore, goethite was more prone to incorporate Al in its structure than was lepidocrocite.

The ferruginous smectite described here as the last product in the alteration process is not unique to Mont Mégantic. Recently, De Kimpe *el al.* (1987) reported iron-rich smectites of similar type and occurrence from Mont Saint-Bruno, Quebec, and showed them to be trioctahedral also, with octahedral vacancies. The ferruginous smectite from Mont Mégantic and Mont Saint-Bruno is considered to be a derivative of saponite and is appropriately described here as a ferric iron-rich saponite or ferrian saponite. Theoretically, such a mineral could be described as a magnesian nontronite; however, complete solid solution has not been reported to date between saponite and nontronite, and a large amount of octahedral Mg in nontronite cannot be reasonably explained from a genetic point of view.

SUMMARY

Saprolite has developed on the intrusive gabbroic rocks between the outer syenite rim and inner granitic core of Mont Mégantic, Quebec. In the outcrop examined in the present study, iron-rich gabbro (ferrogabbro) was extensively altered, with most of the mafic minerals and magnetite decomposing to goethite, lepidocrocite, ferrian saponite, and other iron-rich clay minerals. Felsic minerals were partly altered to kaolinite. These secondary minerals formed in numerous microcracks in the outer shell of boulders and in cracks and fissures in bedrock and subsequently moved to the lower part of the saprolite, along with more resistant primary minerals, such as plagioclase, ilmenite, and apatite.

In addition to ferrian saponite, other iron-rich clay minerals, such as interstratified vermiculite/biotite and ferrian vermiculite were identified, the latter commonly coexisting with the ferrian saponite. The ferrian saponite and the ferrian vermiculite are similar in composition, although the former is slightly richer in SiO_2 and MgO and poorer in Fe_2O_3 than the latter. The principal difference between the identified ferrian saponite and saponite itself, besides iron content, appears to be the moderate number of vacancies in the octahedral sheets of the former. Such structural vacancies and the coexistence of this phase with iron oxyhydroxides suggest that the ferr*ian* saponite might have formed from ferr*oan* saponite by the expulsion of Fe^{3+} from the octahedral sheets of the precursor phase following oxidation of Fe^{2+}.

ACKNOWLEDGMENTS

The authors are grateful to M. Jaakkimainen, R. Rivard, G. C. Scott, R. Guertin, and M. McGrath for their help with the chemical and mineralogical analyses, and to G. J. Ross and C. Wang for reviewing the

manuscript and to F. A. Mumpton, Editor, for improving the text.

REFERENCES

Cardile, C. M. and Johnston, J. H. (1985) Structural studies of nontronites with different iron contents by ^{57}Fe Mössbauer spectroscopy: *Clays & Clay Minerals* **33,** 295–300.

Clark, S. P., Jr. (1966) Composition of rocks: in *Handbook of Physical Constants,* S. P. Clark, Jr., ed., *Geol. Soc. Amer. Memoir* **97,** p. 4.

Clément, P. and De Kimpe, C. R. (1977) Geomorphological conditions of gabbro weathering at Mount Mégantic, Quebec: *Can. J. Earth Sci.* **14,** 2262–2273.

Dejou, J., Clément, P., and De Kimpe, C. R. (1982) Importance du site dans la genèse des minéraux secondaires issus des altérations superficielles. Exemple des granites et gabbros du Mont-Mégantic, Québec, Canada: *Catena* **9,** 181–198.

De Kimpe, C. R., Dejou, J., and Chevalier, Y. (1987) Evolution géochimique superficielle des pyroxénites ignées du Mont Saint-Bruno, Quebec: *Can. J. Earth Sci.* **24,** 760–770.

Delvigne, J., Bisdom, E. B. A., Sleeman, J., and Stoops, G. (1979) Olivines, their pseudomorphs and secondary products. *Pedologie* **29,** 247–309.

Eby, N. (1984) Geochronology of the Monteregian Hills alkaline igneous provenance, Quebec: *Geology* **12,** 468–470.

Farmer, V. C. (1974) The layer silicates: in *The Infrared Spectra of Minerals,* V. C. Farmer, ed., Mineralogical Society, London, 539 pp.

Farmer, V. C., Russell, J. D., MacHardy, W. J., Newman, A. C. D., Ahlrichs, J. L., and Rimsaite, J. Y. H. (1971) Evidence for loss of protons and octahedral iron from oxidized biotites and vermiculites: *Mineral.Mag.* **38,** 121–137.

Kodama, H. (1985) Infrared spectra of minerals: Reference guide to identification and characterization of minerals for the study of soils: *Res. Br. Agriculture Canada Tech Bull.* **1985-1E,** 197 pp.

Kodama, H. and De Kimpe, C. R. (1983) Ferruginous swelling clay minerals in a gabbro saprolite from Mount Mégantic, Quebec: *Can. J. Soil Sci.* **63,** 143–148.

Kohyama, N., Shimoda, S., and Sudo, T. (1973) Iron-rich saponite (ferrous and ferric forms): *Clays & Clay Minerals* **21,** 229–237.

Mehra, O. P. and Jackson, M. L. (1960) Iron oxide removal from soils and clays by a dithionite-citrate system buffered with sodium bicarbonate: in *Clays & Clay Minerals, Proc. 7th Natl. Conf., Washington, D.C., 1958,* Ada Swineford, ed., Pergamon Press, New York, 317–327.

Miyamoto, N. (1957) Iron-rich saponite from Mazé, Niigata Prefecture, Japan: *Mineral. J.* **2,** 193–195.

Moenke, H. (1966) *Mineralspektren. II. Phyllosilikat* (Nontronite): Akademie-Verlag, Berlin, sheet 6.100.

Norrish, K. and Taylor, R. M. (1961) The isomorphous replacement of iron by aluminium in soil goethites: *J. Soil Sci.* **12,** 294–306.

Oinuma, K. and Kayashi, H. (1968) Infrared spectra of clay minerals: *J. Toko Univ. General Educ. (Nat. Sci.)* **9,** 57–98.

Reichen, L. E. and Fahey, J. J. (1962) An improved method for the determination of FeO in rocks and minerals including garnet: *U.S. Geol. Surv. Bull.* **1144-B,** 5 pp.

Reid, A. M. (1976) Rapport sur la géologie du Mont Mégantic: *Minist. Rich. Nat. Québec. Rapport* **ES-25,** 59 pp.

Schwab, R. B. and Küstner, D. (1977) Präzisionsgitterkonstantenbestimmung zur Festlegung röntgenorgraphischer Bestimmungskurven für synthetische Olivine der Mischkristallreihe Forsterit-Fayalit: *N. Jahrb. Mineral. Mh.,* 205–215.

Schwertmann, U. and Taylor, R. M. (1977) Iron oxides: in *Minerals in Soil Environments,* J. B. Dixon and S. B. Weed, eds., Soil Science Society of America, Madison, Wisconsin, 145–180.

Sherman, G. D., Ikawa, H., Uehara, G., and Okazaki, E. (1962) Types of occurrence of nontronite and nontronite-like minerals in soils: *Pacific Science* **16,** 57–62.

Smith, J. V. and Gay, P. (1958) The powder patterns and lattice parameters of plagioclase feldspars II: *Mineral. Mag.* **31,** 744–762.

Sudo, T. (1954) Iron-rich saponite found from Tertiary iron sand beds in Japan: *J. Geol. Soc. Japan* **59,** 18–27.

Sudo, T. and Ota, S. (1952) An iron-rich variety of montmorillonite found in Oya-ishi: *J. Geol. Soc. Japan* **58,** 487–491.

Weaver, C. E. and Pollard, L. D. (1973) *The Chemistry of Clay Minerals:* Elsevier, Amsterdam, 213 pp.

(Received 13 April 1987; accepted 10 August 1987; Ms. 1661)